Role of posterodorsal medial amygdala kisspeptin and urocortin-3 in pubertal timing in female mice

Deyana Ivanova[1], Xiao-Feng Li[1], Yali Liu[2], Caitlin McIntyre[1], Cathy Fernandes[3,4], Geffen Lass[1], Lingsi Kong[1] and Kevin T O'Byrne[1]

[1]Department of Women and Children's Health, Faculty of Life Science and Medicine, King's College London, UK

[2]Department of Assisted Reproduction, Shanghai Ninth People's Hospital, Shanghai Jiaotong University School of Medicine, Shanghai, People's Republic of China.

[3]Social, Genetic & Developmental Psychiatry Centre, Institute of Psychiatry, Psychology & Neuroscience, King's College London, UK

[4] MRC Centre for Neurodevelopmental Disorders, King's College London, UK

Short title: MePD kisspeptin and urocortin-3 role in puberty

Key words: puberty, kisspeptin, psychosocial stress, LH pulsatility, Ucn3, MePD, behaviour

Corresponding author's contact details: Deyana Ivanova (deyana.ivanova@kcl.ac.uk) and Kevin T O'Byrne (kevin.obyrne@kcl.ac.uk), Department of Women and Children's Health, School of Life Course and Population Sciences, Faculty of Life Science and Medicine, King's College London, 2.92W Hodgkin Building, Guy's Campus, London SE1 1UL, UK.

Reprint requests: Deyana Ivanova, Department of Women and Children's Health, School of Life Course Sciences, Faculty of Life Science and Medicine, King's College London, 2.92W Hodgkin Building, Guy's Campus, London SE1 1UL, UK.

Grants supporting paper: The authors gratefully acknowledge the financial support from UKRI: BBSRC (BB/S000550/1) and MRC (MR/N022637/1). DI is a PhD student funded by MRC-DTP studentship at King's College London.

The authors have nothing to disclose.

Abstract

Post-traumatic stress disorder impedes pubertal development and disrupts pulsatile LH secretion. Kisspeptin (kiss1) neurons in the posterodorsal sub-nucleus of the medial amygdala (MePD) are an upstream modulator of the hypothalamic gonadotropin-releasing hormone (GnRH) pulse generator, pubertal timing, as well as emotional processing and anxiety. Psychosocial stress exposure alters neuronal activity within the MePD increasing the expression of Urocortin3 (Ucn3) and its receptor corticotropin-releasing factor type-2 receptor (CRFR2) whilst enhancing the inhibitory output from the MePD to key hypothalamic reproductive centres. We test the hypothesis that psychosocial stress, processed by the MePD, is relayed to the hypothalamic GnRH pulse generator to delay puberty. Firstly, we virally infected Kiss-cre-tdTomato mice with stimulatory DREADDs targeting MePD kiss1 neurons and monitored the effect on pubertal timing. Next, we exposed C57Bl6/J mice to the predator odor, 2,4,5-Trimethylthiazole (TMT), during pubertal transition and examined the effect on pubertal timing, pre-pubertal LH pulses and anxiety-like behaviour. Subsequently, we virally infected Ucn3-cre-tdTomato mice with stimulatory DREADDs targeting MePD Ucn3 neurons and determined the effect on pubertal timing. Activation of MePD kiss1 neurons during pubertal development advanced puberty. Additionally, exposure to TMT during pubertal development delayed puberty, suppressed pre-pubertal LH pulsatility and enhanced anxiety-like behaviour, while activation of MePD Ucn3 neurons delayed puberty. Kiss1 activation in the MePD modulates the maturation of the reproductive axis advancing puberty in female mice. Moreover, early psychosocial stress exposure decreases GnRH pulse generator frequency delaying puberty whilst inducing anxiety-behaviour in female mice, an effect potentially mediated by Ucn3 neurons in the MePD.

48 **Introduction**

49 In humans post-traumatic stress disorder (PTSD) is associated with altered pubertal timing and
50 the development of anxiety disorders (1,2). Predator odor exposure is a classic model for PTSD
51 in rodents (3) and has been shown to delay puberty (4), suppress luteinizing hormone (LH)
52 pulse frequency (5) and inhibit the pre-ovulatory LH surge (6). The gonadotropin-releasing
53 hormone (GnRH) pulse generator that controls the hypothalamus-pituitary-gonadal (HPG) axis
54 and pubertal development is restrained in the juvenile, but reactivated at a critical time point
55 with increased frequency leading to the initiation of puberty (7). However, the neural
56 mechanisms controlling pubertal timing are not fully established.

57 Kisspeptin (kiss1) is known to be a major gatekeeper of pubertal onset. An absence of the
58 *kiss1* gene and kiss1 receptor (kiss1r) in mice and humans leads to a loss of gonadal maturation
59 and a lack of pubertal onset (8,9), and treatment with kisspeptin can reactivate the HPG axis
60 during the juvenile hiatus in monkeys and rats (10,11). Kiss1 neurons are located in the
61 anteroventral periventricular nucleus (AVPV) and arcuate nucleus (ARC) of the hypothalamus
62 in mice (12). The ARC kiss1 neurons, known as KNDy because they co-express neurokinin B
63 (NKB) and dynorphin A (Dyn), are a critical component of the GnRH pulse generator (12–14).
64 The activation of KNDy neurons induces pulsatile release of kiss1 acting on GnRH dendrons
65 in the median eminence to stimulate pulsatile GnRH secretion (15). The AVPV kiss1 neurons
66 project to GnRH cell bodies and proximal dendrites and are known to control the preovulatory
67 LH surge and ovulation in rodents (16). In the juvenile, a neurobiological break exerted on the
68 ARC GnRH pulse generator suppresses pulsatile kiss1 release in the median eminence,
69 however the nature of this upstream inhibition of the GnRH pulse generator, which is released
70 at the end of the juvenile phase to trigger puberty is unknown (7).

71 The amygdala, a stress-sensitive part of the limbic brain, is involved in processing anxiety and
72 fear as well as modulating pubertal timing and the HPG axis. Lesioning of the amygdala

73 advances menarche in female rhesus macaques (17), whereas electrical stimulation of this
74 region delays puberty in rats (18). Specific lesioning of the posterodorsal sub-nucleus of the
75 medial amygdala (MePD) advances puberty in rats (19), suggesting this region may play a key
76 role in exerting an inhibitory break on pubertal timing. The MePD sends GABAergic
77 projections to various hypothalamic reproductive centres (20,21) and has been shown to project
78 directly to ARC KNDy neurons, although their neurochemical phenotype is undetermined
79 (22,23). Interestingly, the MePD contains a kiss1 neuronal population (24) and antagonism of
80 MePD kiss1 delays puberty, disrupts estrous cyclicity and the LH surge in rats (25). Selective
81 optogenetic stimulation of MePD kiss1 neurons increases LH pulse frequency in adult mice
82 (26) however, it is unknown whether pre-pubertal activation of MePD kiss1 neurons may be
83 involved in driving puberty onset. Moreover, the MePD is highly responsive to psychosocial
84 stress, exhibiting a distinct firing pattern in response to predator odor (27) and recently cat odor
85 was found to delay puberty, disrupt estrous cyclicity and induce a fear response in rats (4). The
86 MePD may be a central hub involved in the integration of external olfactory and anxiogenic
87 signals with the GnRH pulse generator.

88 Central administration of the stress neuropeptide corticotrophin releasing factor (CRF) dose-
89 dependently delays puberty, while CRF-receptor antagonism advances puberty in rats (28).
90 Urocortin-3 (Ucn3), a member of the CRF family and an endogenous ligand for CRF type 2
91 receptors (CRFR2) is found in abundance in the MePD (29). Psychosocial stressors, including
92 social defeat and restraint, increase cfos expression in CRFR2 positive neurons and increase
93 Ucn3 mRNA expression in the MePD of rodents (30). Moreover, we have recently shown that
94 MePD Ucn3 mediates predator odor and restraint stress-induced suppression of pulsatile LH
95 secretion in mice (5).

96 In this study, we aimed to determine whether MePD kiss1 neurons are involved in modulating
97 pubertal timing. We also tested the hypothesis that predator odor stress suppresses pre-pubertal

98 LH pulse frequency and delays pubertal timing. Additionally, we assessed social, anxiety and
99 fear-like behaviour as measures of psychosocial stress in predator odor-exposed pre-pubertal
100 female mice. Finally, we aimed to determine whether MePD Ucn3 signalling is involved in
101 modulating pubertal timing.

102 **Methods**

103 **Mice**

104 Breeding pairs of C57Bl6/J mice were purchased from Charles River Laboratories
105 International, Inc. Breeding pairs of heterozygous transgenic Kiss-cre mice (strain
106 129S6Sv/Ev) were obtained from the Department of Physiology, Development and
107 Neuroscience, University of Cambridge, UK. Genotyping of Kiss-cre mice was performed
108 using PCR to detect heterozygosity. Heterozygous Kiss-cre mice were bred with cre-activated
109 tdTomato reporter mice to obtain Kiss-cre-tdTomato mice, as previously described (31). For
110 Ucn3-cre mice, cryopreserved sperm of strain (Tg(Ucn3-cre)KF43Gsat/Mmucd; congenic on
111 C57BL/6 background) was acquired from MMRRC GENSAT. Breeding pairs of heterozygous
112 transgenic Ucn3-cre mice were recovered by insemination of female C57Bl6/J mice at King's
113 College London. Genotyping of Ucn3-cre mice was performed using PCR to detect
114 heterozygosity. Heterozygous Ucn3-cre mice were bred with cre-activated tdTomato reporter
115 mice (strain B6.Cg-Gt(ROSA)26Sortm9(CAG-tdTomato)Hze/J; congenic on C57BL/6
116 background obtained from The Jackson Laboratory, Bar Harbor, ME, USA) to obtain Ucn3-
117 cre-tdTomato mice, as previously described (5,29). Litter size was reduced to 6-8 pups 2-3
118 days after birth (on pnd 2-3) to standardise body weight, which can alter pubertal development.
119 Mice aged between 21 to 45 days were group housed in individually ventilated cages equipped
120 with wood-chip bedding and nesting material with food and water ad libitum and sealed with
121 a HEPA-filter at 25 ± 1 °C in a 12:12 h light/dark cycle, lights on at 07:00 h. All procedures

122 were carried out following the United Kingdom Home Office Regulations and approved by the
123 Animal Welfare and Ethical Review Body Committee at King's College London.

124 **Stereotaxic adeno-associated-virus injection**

125 All surgical procedures were carried out with aseptic conditions and under general anaesthesia
126 using ketamine (Vetalar, 100 mg/kg, i.p.; Pfizer, Sandwich, UK) and xylazine (Rompun, 10
127 mg/kg, i.p.; Bayer, Leverkusen, Germany). The mouse brain atlas of Paxinos and Franklin
128 (32) was used to obtain target coordinates for the MePD (2.15 mm lateral, -1.25 mm from
129 bregma, at a depth of -5.30 mm below the skull surface) of pre-pubertal mice. Mice at pnd 14
130 were temporarily taken from their mother and secured in a David Kopf stereotaxic frame (Kopf
131 Instruments), a small skin incision was made to reveal the skull and two small holes were
132 drilled above the location of the MePD. Bilateral stereotaxic viral injections of the stimulatory
133 adeno-associated-virus (AAV) carrying the DIO-hM3D-mCitrine, DREADD, construct
134 (AAV-hSyn-DIO-HA-hM3D(Gq)-IRES-mCitrine, $3x10^{11}$ GC/ml, Serotype:5; Addgene) was
135 administered intra-MePD using the robot stereotaxic system (Neurostar, Tubingen, Germany),
136 performed for the targeted expression of DIO-hM3D-mCitrine in MePD kiss1 neurons in Kiss-
137 cre-tdTomato mice and MePD Ucn3 neurons in Ucn3-cre-tdTomato mice. AAV-hSyn-DIO-
138 HA-hM3D(Gq)-IRES-mCitrine (150 nl) was bilaterally injected into the MePD using a 2-µl
139 Hamilton micro syringe (Esslab, Essex, UK) over 10 min and the needle was left in position
140 for a further 5 min then slowly lifted over 2 min. Mice that were cre-positive received the
141 AAV-hM3D injection (test mice) or a control virus AAV-YFP (Addgene) (control mice) where
142 the control virus does not contain the DIO-hM3D-mCitrine construct. The mice were placed
143 back with the mother for a further 7 days until wean day (pnd 21). Ten Kiss-cre-tdTomato
144 mice received the AAV-hM3D injection and 5 Kiss-cre-tdTomato mice received the control
145 AAV-YFP. Nine Ucn3-cre-tdTomato mice received the AAV-hM3D injection and 6 Ucn3-
146 cre-tdTomato mice received the control AAV-YFP.

147 **Chronic pre-pubertal predator-odor exposure and puberty evaluation**

148 Female pups were weaned on pnd 21 and separated into control and test groups. To investigate
149 the effects of chronic pre-pubertal psychosocial stress mice were removed from their home
150 cages, singly housed in new cages and left to habituate for 10 min. After the habituation period,
151 the mice were exposed to 12 µl of 2,4,5-Trimethylthiazole (TMT; synthetic extract of fox urine;
152 ≥98% purity; Sigma-Aldrich, UK) pipetted on a small circular piece of filter paper in a petri
153 dish placed in the centre of the cage for 20 min. The mice were exposed to TMT daily, at
154 random time points, for 14 days (from pnd 21 to 35). Control mice were exposed to filter paper
155 soaked with 12 µl of ddH_2O water. To rule out the possibility that physiological and
156 behavioural responses in TMT-exposed mice resulted from novelty of scent we repeated the
157 experiment with 85 mM of ethyl vanillin (≥98% purity; Sigma-Aldrich UK) as a control scent
158 in a separate cohort of mice. Mice were monitored from pnd 24 for vaginal opening (VO) and
159 first estrous (FE) indicated by epithelial cell cornification. Once the occurrence of VO was
160 detected, vaginal smears were taken to determine the exact day of FE.

161 **Pre-pubertal blood sampling**

162 The effect of TMT exposure on pre-pubertal LH pulses was measured, on pnd 26 and 29. Mice
163 were handled twice daily for 10 min to habituate to tail-tip blood collection for at least 7 days
164 prior to blood sampling, as described previously (5). For LH measurement, 3 µl of blood was
165 collected every 5 min for 80 min. Blood sampling was performed on pnd 26 and 29 during the
166 period of daily TMT exposure (pnd 21-35). Blood samples were collected at least 2 h before
167 TMT-exposure on these days. Blood collection was performed between 09:00-12:00 h.

168 **Behavioural tests**

169 ***Light Dark Box***

170 Mice were transported to a new room (lights off) and left to habituate for 30 min. Mice were
171 placed in the centre of the light compartment facing towards the dark compartment. The time
172 spent in each compartment (entry with all 4 limbs) was recorded manually over a period of 5
173 min by two independent observers. The LDB test was carried out on pnd 19, 27 and 40.
174 Behaviour testing performed during the period of daily TMT exposure (pnd 21-35) and was
175 measured before the exposure to TMT on that day. This applies to all behaviour tests
176 performed during the TMT exposure period. All behaviour tests were performed between
177 11:00-13:00 h.

178 ***Social interaction with familiar conspecific***

179 Mice were transported to a new dimly lit room and left to habituate for 30 min. Experimental
180 mice and a same sex familiar conspecific (similar age, weight and strain) were placed
181 simultaneously into the test arena (a new cage with clean wood-chip bedding). The time spent
182 following, sniffing, grooming and mounting the conspecific was monitored and recorded
183 manually over a period of 5 min by two independent observers. The social interaction test was
184 carried out on pnd 19, 27 and 40.

185 ***Elevated Plus maze***

186 Mice were transported to a new room (lights on) and left to habituate for 30 min. Mice were
187 placed in the centre of the maze facing towards the closed arms. The time spent in each part
188 of the maze (open, centre and closed; entry with all 4 limbs) was recorded manually over a
189 period of 5 min by two independent observers. The EPM test was carried out on pnd 20, 28
190 and 41.

191 **Chronic DREADD activation of kiss1 or Ucn3 neurons in the MePD**

192 For DREADDs experiments, stock solution of Clozapine-N-oxide (CNO) was made by
193 dissolving 5 mg of CNO in 1 ml of 0.9% sterile saline solution and stored at 4 °C. CNO was
194 made fresh daily and administered via drinking water at a final concentration of 0.5 mg CNO/
195 kg, as described previously (33) for 14 days from pnd 21-35. Mice were monitored from pnd
196 22 for vaginal opening (VO) and first estrous (FE), as described above.

197 **Validation of AAV injection**

198 On pnd 50, Kiss-cre-tdTomato and Ucn3-cre-tdTomato mice were anaesthetised with a lethal
199 dose of ketamine. Transcardial perfusion was performed with heparinised saline for 5 min
200 followed by ice-cold 4% paraformaldehyde (PFA) in phosphate buffer (pH 7.4) for 15 min
201 with a pump (Minipuls, Gilson, Villiers Le Bel, France). Brains were immediately collected
202 and fixed in 15% sucrose in 4% PFA at 4 °C and left to sink. Brains were then transferred to
203 30% sucrose in phosphate-buffered saline (PBS) and left to sink. Brains were snap-frozen in
204 isopropanol on dry ice and stored in -80°C. Every third coronal brain section, 30-µm/section,
205 was collected using a cryostat (Bright Instrument Co., Luton, UK) through-out the MePD
206 region corresponding to -1.34 mm to -2.70 mm from bregma. Brain sections were mounted on
207 microscope slides, air dried and covered with ProLong Antifade mounting medium (Molecular
208 Probes, Inc. OR, USA). The number of tdTomato labelled and AAV-hM3D-mCitrine infected
209 kiss1 or Ucn3 neurons per side per slice in the MePD was quantified from 4 slices. For AAV-
210 hM3D-mCitrine injected Kiss-cre-tdTomato or Ucn3-cre-tdTomato mice we determined
211 whether kiss1 or Ucn3 neurons were infected in the MePD region by merging td-Tomato
212 fluorescence of kiss1 or Ucn3 neurons with mCitrine fluorescence in the MePD. Images were
213 taken using Axioskop 2 Plus microscope (Carl Zeiss) equipped with axiovision, version 4.7
214 (Carl Zeiss). Only data from animals with correct AAV injection were analysed.

215 **LH pulse detection and analysis**

216 Blood samples were processed with a LH ELISA, as previously reported (34). Capture
217 antibody (monoclonal antibody, anti-bovine LHβ subunit, AB_2665514) was purchased from
218 Department of Animal Science at the University of California, Davis. Mouse LH standard
219 (AFP-5306A) and primary antibody (polyclonal antibody, rabbit LH antiserum, AB_2665533)
220 were obtained from Harbour-UCLA (California, USA). Secondary antibody (Horseradish-
221 Peroxidase (HRP)-linked donkey anti-rabbit IgG polyclonal antibody, AB_772206) was
222 purchased from VWR International (Leicestershire, UK). Inter-assay and intra-assay
223 variations were 4.6% and 10.2%, respectively. ODs of the standards were plotted against the
224 log of the standard concentrations, non-linear regression to fit the points and parameters were
225 extracted to calculate the concentration of LH (ng/ml) in blood samples, as previously
226 described (34). The LH concentration at every time point of blood collection was plotted as a
227 line and scatter graph using Igor Pro 7, Wavemetrics, Lake Oswego, OR, USA. DynPeak
228 algorithm was used for the detection of LH pulses (35).

229 **Statistics**

230 For TMT-exposed and DREADD injected female pre-pubertal mice, data obtained for VO and
231 FE was analysed using RM one-way ANOVA. Data obtained for performance on LDB, SI and
232 EPM, LH pulse frequency and body weight measure were analysed using RM two-way
233 ANOVA. Statistics were performed using Igor Pro 7, Wavemetrics, Lake Oswego, OR, USA.
234 Data was represented as mean ± SEM and +$p<0.05$, ++$p<0.001$ and +++$p<0.0001$ were
235 considered to be significant.

236 **Results**

237 **Selective DREADD activation of kiss1 neurons in the MePD advances puberty onset**

238 Bilateral DREADD activation of MePD kiss1 neurons during the pubertal transition period,
239 pnd 21 to 35, of Kiss-cre-tdTomato mice advanced FE without altering VO compared to non-
240 surgery and AAV-YFP controls (Fig. 1, A and B; Control vs DREADD, +$p<0.05$; DREADD,
241 n=8, control AAV, n=5, no surgery, n=5). Data for non-surgery and control AAV-YFP injected
242 mice were combined as control since there was no significant difference between the two
243 control groups. Body weight was unaffected between the experimental groups (Fig. 1, C;
244 Control vs DREADD). The data from this study shows that activation of MePD kiss1 during
245 the pubertal transition advances pubertal timing. Mice with misplaced injections (n=2) were
246 excluded from the analysis.

247 **Chronic TMT exposure delays puberty onset**

248 TMT exposure during the pubertal transition period, pnd 21 to 35, delayed FE without altering
249 VO compared water and ethyl vanillin controls (Fig. 2, A and B; Control vs TMT,
250 +++$p<0.0001$; TMT, n=14, water control, n=6, ethyl vanillin control, n=4). Data for water and
251 ethyl vanillin exposed control mice were combined as control since there was no significant
252 difference between the two control groups. Body weight was unaffected between the
253 experimental groups (Fig. 2, C; Control vs TMT). The data from this study shows that
254 predator-odor stress exposure during the pubertal transition delays pubertal onset.

255 **Chronic TMT exposure decreases pre-pubertal LH pulse frequency**

256 TMT exposure during the pubertal transition period, pnd 21 to 35, suppressed pre-pubertal LH
257 pulse frequency on pnd 26 and 29 compared to water and ethyl vanillin controls (Fig. 3, A-E;
258 Control vs TMT, ++$p<0.001$; TMT, n=8, water control, n=6, ethyl vanillin control, n=3). On

259 pnd 29, the average LH pulse frequency for the control group tended to increase compared to
260 the control group on pnd 26 potentially marking an acceleration of GnRH pulse generator
261 activity approaching the onset of puberty (Fig. 3, A, C and E). The results of this experiment
262 are summarised in the figure 3E. Data for water and ethyl vanillin exposed control mice were
263 combined as control since there was no significant difference between the two control groups.
264 The data from this study shows that predator-odor stress exposure during the pubertal transition
265 inhibits pre-pubertal LH pulsatility.

266 **Chronic TMT exposure induced long-lasting anxiety and fear-like behaviour**

267 We investigated anxiety and fear-like behaviour induced by TMT-exposure during the pubertal
268 transition period, pnd 21 to 35. Anxiety and fear-behaviour were assessed using standard
269 anxiety and fear tests, the LDB, SI and EPM, on pnd 19 or 20 (prior to day of weaning and
270 TMT-exposure), pnd 27 or 28 (during the TMT exposure period) and pnd 40 or 41 (a week
271 after termination of TMT-exposure). The first LDB, SI and EPM trial on pnd 19 or 20, prior
272 to weaning, confirms no group difference in anxiety before the beginning of TMT-exposure
273 (Fig. 4, A-C). TMT-exposed mice spent significantly less time in the light compartment of the
274 LDB as well as socialising with a familiar conspecific compared to the control group on pnd
275 27, but not on pnd 40 (Fig. 4, A, B; Control vs TMT, +$p<0.05$; TMT, n=14, water control, n=6,
276 ethyl vanillin control, n=4). TMT-exposed mice spent less time in the open arms of the EPM
277 on pnd 28 and pnd 41 compared to controls (Fig. 4, C; Control vs TMT, ++$p<0.001$; TMT,
278 n=14, water control, n=6, ethyl vanillin control, n=4). It is acknowledged that repeat testing
279 on the EPM assesses phobia/fear (36). On pnd 20, pnd 28 and 41, within-group analysis
280 showed no significant differences in the total time spent in the open arms of the EPM across
281 the different test days in the control group. However, within-group analysis of the TMT-
282 exposed group showed a significant difference in time-spent in the open arm of the EPM on

283 pnd 41 compared to pnd 28 (Fig. 4, C; TMT on pnd 28 vs TMT on pnd 41, ###p<0.0001).

284 TMT-exposure during pubertal transition had a long-lasting effect on anxiety and fear/phobia.

285 **Selective DREADD activation of Ucn3 neurons in the MePD delays puberty onset**

286 Bilateral DREADD activation of MePD Ucn3 neurons during the pubertal transition period,
287 pnd 21 to 35, of Ucn3-cre-tdTomato mice delayed FE without altering VO compared to non-
288 surgery and AAV-YFP controls (Fig. 5, A and B; Control vs DREADD, +$p<0.05$; DREADD,
289 n=8, control AAV, n=6, no surgery, n=4). Data for non-surgery and control AAV-YFP injected
290 mice were combined as control since there was no significant difference between the two
291 control groups. Body weight was unaffected between the experimental groups (Fig. 5, C;
292 Control vs DREADD). These data show that activation of MePD Ucn3 during the pubertal
293 transition delays pubertal timing. Mice with misplaced injections (n=1) were excluded from
294 the analysis

295 **Selective expression of DREAD(Gq) in MePD kiss1 and Ucn3 neurons**

296 Evaluation of m-Citrine, hM3D, expression in tdTomato labelled neurons from AAV-injected
297 Kiss-cre-tdTomato mice revealed that 78 ± 3% of MePD Kiss neurons expressed hM3D and
298 the number of tdTomato labelled kiss1 neurons per side per slice in the MePD was counted at
299 7.38 ± 1.66 (mean ± SEM) with the number of AAV-hM3D-mCitrine infected neurons being
300 5.78 ± 1.42 (mean ± SEM) (n=8). A representative example is shown in Fig 6, A-F. Evaluation
301 of m-Citrine, hM3D, expression in tdTomato labelled neurons from AAV-injected Ucn3-cre-
302 tdTomato mice revealed that 86 ± 5% of MePD Ucn3 neurons expressed hM3D and the number
303 of tdTomato labelled Ucn3 neurons per side per slice in the MePD was counted at 72.90 ± 5.48
304 (mean ± SEM) with the number of AAV-hM3D-mCitrine infected neurons being 63.00 ± 6.83
305 (mean ± SEM) (n=8). A representative example is shown in Fig 7, A-F.

306 **Discussion**

307 The present study shows for the first time that DREADD activation of MePD kiss1 neurons
308 from weaning on pnd 21 for 14 days advances puberty onset, revealing a crucial stimulatory
309 role of MePD kiss1 signalling in regulating the HPG axis during puberty. Additionally, chronic
310 exposure to the psychogenic stressor, predator odor, from pnd 21 for 14 days suppresses the
311 pubertal acceleration of LH pulse frequency, delaying puberty onset, whilst concurrently
312 inducing long-lasting anxiety and fear-like behaviour. Moreover, DREADD activation of
313 MePD Ucn3 neurons during this same developmental period delays puberty onset,
314 demonstrating that MePD Ucn3 signalling may play an important role in stress-related changes
315 in pubertal timing.

316 Hypothalamic kiss1 signalling is pivotal in regulating puberty onset in various species,
317 including rodents and humans (7,11). Pubertal onset is thought to be timed by an increase in
318 GnRH pulse generator frequency, however the mechanisms underlying the timing of ARC
319 kiss1 neuronal activation to trigger pubertal onset are not well established. The amygdala is
320 known to influence pubertal timing in primates (17), but more specifically, the MePD has been
321 shown to regulate pubertal timing and reproductive function in rodents (4,19), vis-à-vis MePD
322 kiss1 receptor antagonism delays puberty, reduces the occurrence of preovulatory LH surges
323 in rats (25) and MePD kiss1 neuronal activation heightens sexual partner preference in male
324 mice (37). Recently, we have shown optogenetic stimulation of MePD kiss1 neurons increases
325 GnRH pulse generator frequency in adult female mice (26), and in the present study we show
326 that DREADD activation of MePD kiss1 neurons during the critical pubertal development
327 period advances FE without affecting VO or body weight in female mice. In mice, VO and FE
328 do not coincide, wherein VO is not tightly coupled to the first ovulation, but rather a variable
329 time gap exists between VO and FE; the latter associated with first ovulation and considered
330 the unequivocal marker of puberty (38). Although the present study clearly shows an

331 advancement of puberty onset following activation of MePD kiss1 neurons, the underlying
332 neural networks engaged remain to be established.

333 In mice, the maturation of the kiss1 system begins with an increase in the number of
334 hypothalamic kiss1 neurons in peripubertal mice (39) occurring concomitantly with an increase
335 in connectivity between kiss1 and GnRH neurons which is considered critical for normal
336 puberty onset (40). Kiss1 expression in the rostral periventricular area of the third ventricle
337 increases across the pubertal transition in mice (41) and knockdown of AVPV kiss1 delays
338 puberty and reduces the occurrence of LH surges (42). In ovine species, exposure to a sexually
339 active ram can advance puberty (43) and stimulate ovulation in anoestrous ewes via the
340 resurgence of pulsatile and surge release of LH coinciding with elevated cfos expression in
341 kiss1 neurons of the ARC, pre-optic area (POA) and medial amygdala (44,45). MePD kiss1
342 neurons have been shown to project directly to GnRH neurons in the medial POA (46), hence
343 revealing a possible route via which MePD kiss1 neurons may control puberty. However,
344 puberty onset has been associated with increased ARC Tac2 (encoding NKB) and kiss1 mRNA
345 expression in mice (47,48), which are critical components of the GnRH pulse generator.
346 Moreover, there is an increase in ARC kiss1 promoter activity during pubertal development
347 (49). We know direct neural projections, of unknown phenotype, extend from the MePD to
348 ARC kiss1 neurons (22,23) and MePD kiss1 signalling functions as an upstream regulator of
349 the ARC KNDy network, accelerating GnRH pulse generator frequency (26,50). Therefore,
350 an alternative route may involve upstream MePD kiss1 signalling accelerating ARC KNDy
351 neuronal activity to trigger pubertal onset.

352 Stress exposure during the juvenile period is known to alter pubertal timing and induce anxiety
353 behaviour in mammals, including rodents, primates and humans (1,2,4,51). Predator odor
354 exposure in rodents is a model for PTSD; increasing fear and anxiety behaviour as well as
355 reducing social interaction (3). Previously, we have shown that acute TMT exposure

356 suppresses LH pulsatility (5) and restraint stress, another psychological stressor, inhibits LH
357 pulse frequency while reducing ARC kiss1 cfos expression in adult mice (52). Moreover, we
358 have shown that cat odor delays puberty and induces a fear response in rats (4). In the present
359 study we show that the predator odor, TMT, reduces LH pulsatility and delays puberty in mice.
360 Pre-pubertal LH pulse frequency in the control group tended to increase potentially marking
361 the acceleration of the GnRH pulse generator as the time of puberty onset approaches.
362 Contrastingly, pre-pubertal LH pulse frequency in the TMT-exposed group was significantly
363 lower compared to controls and we did not observe an increase in GnRH pulse generator
364 activity between pnd 26 and 29.

365 Puberty is a sensitive period where enhanced neuroplasticity provides a context for the impact
366 of stress on the development of long-term anxiety disorders in humans (53). Early-life stress
367 increases anxiety-like behaviour in juvenile and adult mice linked to hyper-connectivity
368 between fronto-limbic circuits, involving the amygdala (54). The medial amygdala is activated
369 in response to external stressors and electrophysiological recordings reveal that predator urine
370 robustly activates the MePD, which is associated with delaying pubertal onset (4) and
371 supressing LH pulsatility in rodents (5,55). We found that predator odor-induced pubertal
372 delay was accompanied by increased anxiety-like behaviour, with mice spending significantly
373 less time in the light compartment of the LDB and in the open arms of the EPM during stress
374 exposure. Moreover, we observed that mice exposed to TMT exhibited long lasting fear-like
375 behaviour where they spent significantly less time in the open arm of the EPM compared to
376 controls on pnd 41; 6 days after termination of stress exposure. This is consistent with our
377 previous studies showing rats exposed to cat odor during pubertal development display
378 increased long-lasting fear-like behaviour on the EPM even after the termination of stress
379 exposure (4). Moreover, exposure to fox odor induces long-lasting anxiety on the EPM in rats
380 (56), while mice exposed to foot-shock stress during adolescence exhibit increased startle

381 reflexes into adulthood indicative of lasting anxiety-like behaviour (57). Additionally, TMT-
382 exposed mice showed significantly reduced social interaction with familiar con-specifics
383 during stress exposure whereas sociability tended to increase along with reproductive
384 maturation in the control group, which is consistent with our previous observations where
385 exposure to cat odor during puberty decreased sociability in rats (4).

386 Central administration of CRF inhibits kiss1 expression in the ARC and POA in rats (58). In
387 women with functional hypothalamic amenorrhea there is a correlation between decreased
388 serum kisspeptin and increased CRF concentrations (59). Moreover, an endogenous CRF tone
389 regulates pubertal timing where central administration of CRF in pnd 28 rats delays puberty
390 onset and administration of astressin-B, a CRFR1 antagonist, advances puberty (28). Central
391 antagonism of CRFR2 blocks the suppressive effect of stress on LH pulsatility in rodents (60).
392 These data indicate stress neuropeptides may provide an inhibitory tone on the timing of
393 puberty. Predator odor activates CRFR2 positive neurons in the medial amygdala of rats (61)
394 and we have recently shown that TMT-induced suppression of LH pulsatility is mediated by
395 MePD Ucn3 and CRFR2 signalling in mice (5). In the present study, selective activation of
396 MePD Ucn3 neurons during pubertal development delayed puberty, demonstrating that MePD
397 Ucn3 signalling plays a major role in regulating pubertal timing. The MePD has a major
398 GABAergic output to key hypothalamic reproductive nuclei (21,62) and we know the
399 amygdala exerts an inhibitory brake on pubertal timing (19,63). Ucn3 neurons in the medial
400 amygdala have an interneuron-like appearance (64) where Ucn3 fibres overlap with CRFR2
401 expression (65,66) and we have shown that antagonism of MePD CRFR2 blocks the
402 suppressive effect of TMT on LH pulses in adult mice (5), thus Ucn3 neurons possibly connect
403 to and signal via CRFR2 within the MePD. Moreover, the majority of MePD CRFR2 neurons
404 co-express GAD65 and 67 (29) indicating they are GABAergic and may be involved in
405 mediating stress-induced suppression of the GnRH pulse generator (5). MePD Ucn3 activity

406 modulates puberty possibly via enhancing GABAergic output whilst suppressing kiss1
407 signalling within the MePD, as antagonism of kisspeptin receptor signalling in the MePD
408 decreases GnRH pulse generator frequency (50) while delaying puberty (25).

409 Our findings show for the first time that MePD kiss1 signalling plays a fundamental role in
410 controlling pubertal timing. Moreover, early life exposure to a psychosocial stressor disrupts
411 GnRH pulse generator frequency to delay puberty, and Ucn3 signalling in the MePD may be
412 involved in mediating this response. These findings provide novel insight into the key
413 interactions between the emotional stress centres and reproductive centres in the brain that
414 control pubertal onset in response to the external environment. Alterations in the timed onset
415 of puberty has major implications later in life with increased risk of diverse adverse outcomes,
416 including cancer, gynaecologic/obstetric, cardio-metabolic and neuro-cognitive categories in
417 humans (67). Understanding the mechanisms involved in controlling pubertal timing and the
418 impact of stress is crucial to ultimately aid future development of more effective treatments for
419 stress-related disorders of puberty.

420 **Bibliography**

421 1. Ponnapakkam A, Gensure R. Effects of stress after Hurricanes Katrina and Rita on
422 pubertal disorders in children. Ochsner J. 2008;8(3):129–33.
423 2. Gur RE, Moore TM, Rosen AF, Barzilay R, Roalf DR, Calkins ME, Ruparel K, Scott
424 JC, Almasy L, Satterthwaite TD, Shinohara RT . Burden of Environmental Adversity
425 Associated with Psychopathology, Maturation, and Brain Behavior Parameters in
426 Youths. JAMA Psychiatry. 2019;76(9):966–75.
427 3. Zoladz PR, Diamond DM . Predator-based psychosocial stress animal model of PTSD:
428 Preclinical assessment of traumatic stress at cognitive, hormonal, pharmacological,
429 cardiovascular and epigenetic levels of analysis. Exp Neurol. 2016;284(Pt B):211–9.

430 4. Li XF, Adekunbi DA, Alobaid HM, Li S, Pilot M, Lightman SL, O'Byrne KT . Role
431 of the posterodorsal medial amygdala in predator odour stress-induced puberty delay
432 in female rats. J Neuroendocrinol. 2019;31(6):e12719.
433 5. Ivanova D, Li XF, McIntyre C, Liu Y, Kong L, O'Byrne KT . Urocortin3 in the
434 Posterodorsal Medial Amygdala Mediates Stress-induced Suppression of LH
435 Pulsatility in Female Mice. Endocrinology. 2021;162(12):bqab206.
436 6. Wagenmaker ER, Moenter SM. Exposure to acute psychosocial stress disrupts the
437 luteinizing hormone surge independent of estrous cycle alterations in female mice.
438 Endocrinology. 2017;158(8):2593–602.
439 7. Terasawa E, Guerriero KA, Plant TM. Kisspeptin and Puberty in Mammals. Adv Exp
440 Med Biol. 2013;784:253–73.
441 8. De Roux N, Genin E, Carel JC, Matsuda F, Chaussain JL, Milgrom E.
442 Hypogonadotropic hypogonadism due to loss of function of the KiSS1-derived peptide
443 receptor GPR54. Proc Natl Acad Sci U S A. 2003;100(19):10972–6.
444 9. Seminara SB, Messager S, Chatzidaki EE, Thresher RR, Acierno Jr JS, Shagoury JK,
445 Bo-Abbas Y, Kuohung W, Schwinof KM, Hendrick AG, Zahn D . The GPR54 gene as
446 a regulator of puberty. N Engl J Med. 2003;349(17):1614–27.
447 10. Plant TM, Ramaswamy S, DiPietro MJ. Repetitive activation of hypothalamic G
448 protein-coupled receptor 54 with intravenous pulses of kisspeptin in the juvenile
449 monkey (Macaca mulatta) elicits a sustained train of gonadotropin-releasing hormone
450 discharges. Endocrinology. 2006;147(2):1007–13.
451 11. Navarro VM, Fernandez-Fernandez R, Castellano JM, Roa J, Mayen A, Barreiro ML,
452 Gaytan F, Aguilar E, Pinilla L, Dieguez C, Tena-Sempere M . Advanced vaginal
453 opening and precocious activation of the reproductive axis by KiSS-1 peptide, the
454 endogenous ligand of GPR54. J Physiol. 2004;561(2):379–86.

455 12. Clarkson J, Han SY, Piet R, McLennan T, Kane GM, Ng J, Porteous RW, Kim JS,
456 Colledge WH, Iremonger KJ, Herbison AE. Definition of the hypothalamic GnRH
457 pulse generator in mice. Proc Natl Acad Sci U S A. 2017;114(47):e10216–23.
458 13. Qiu J, Nestor CC, Zhang C, Padilla SL, Palmiter RD, Kelly MJ, Rønnekleiv OK .
459 High-frequency stimulation-induced peptide release synchronizes arcuate kisspeptin
460 neurons and excites GnRH neurons. Elife. 2016;5:e16246.
461 14. Voliotis M, Li XF, De Burgh R, Lass G, Lightman SL, O'Byrne KT, Tsaneva-
462 Atanasova K . The Origin of GnRH pulse generation: An integrative mathematical-
463 experimental approach. J Neurosci. 2019;39(49):9738–47.
464 15. Liu X, Yeo SH, McQuillan HJ, Herde MK, Hessler S, Cheong I, Porteous R, Herbison
465 AE . Highly redundant neuropeptide volume co-transmission underlying episodic
466 activation of the gnrh neuron dendron. Elife. 2021;10:e62455.
467 16. Wang L, Moenter SM. Differential Roles of Hypothalamic AVPV and Arcuate
468 Kisspeptin Neurons in Estradiol Feedback Regulation of Female Reproduction.
469 Neuroendocrinology. 2020;110(3–4):172–84.
470 17. Stephens SBZ, Raper J, Bachevalier J, Wallen K. Neonatal amygdala lesions advance
471 pubertal timing in female rhesus macaques. Psychoneuroendocrinology. 2015;51:307–
472 17.
473 18. Bar-Sela M, Critchlow V. Delayed puberty following electrical stimulation of
474 amygdala in female rats. Am J Physiol. 1966;211(5):1103–7.
475 19. Li XF, Hu MH, Hanley BP, Lin YS, Poston L, Lightman SL, O'Byrne KT . The
476 posterodorsal medial amygdala regulates the timing of puberty onset in female rats.
477 Endocrinology. 2015;156(10):3725–36.
478 20. Choi GB, Dong HW, Murphy AJ, Valenzuela DM, Yancopoulos GD, Swanson LW,
479 Anderson DJ . Lhx6 delineates a pathway mediating innate reproductive behaviors

480 from the amygdala to the hypothalamus. Neuron. 2005;46(4):647–60.
481 21. Keshavarzi S, Sullivan RKP, Ianno DJ, Sah P. Functional properties and projections of
482 neurons in the medial amygdala. J Neurosci. 2014;34(26):8699–715.
483 22. Moore AM, Coolen LM, Lehman MN. Kisspeptin/Neurokinin B/Dynorphin (KNDy)
484 cells as integrators of diverse internal and external cues: evidence from viral-based
485 monosynaptic tract-tracing in mice. Sci Rep. 2019;9(1):1–5.
486 23. Yeo SH, Kyle V, Blouet C, Jones S, Colledge WH. Mapping neuronal inputs to Kiss1
487 neurons in the arcuate nucleus of the mouse. PLoS One. 2019;14(3):e0213927.
488 24. Kim J, Semaan SJ, Clifton DK, Steiner RA, Dhamija S, Kauffman AS. Regulation of
489 Kiss1 expression by sex steroids in the amygdala of the rat and mouse. Endocrinology.
490 2011;152(5):2020–30.
491 25. Adekunbi DA, Li XF, Li S, Adegoke OA, Iranloye BO, Morakinyo AO, Lightman SL,
492 Taylor PD, Poston L, O'Byrne KT . Role of amygdala kisspeptin in pubertal timing in
493 female rats. PLoS One. 2017;12(8):e0183596.
494 26. Lass G, Li XF, de Burgh RA, He W, Kang Y, Hwa-Yeo S, Sinnett-Smith LC,
495 Manchishi SM, Colledge WH, Lightman SL, O'Byrne KT . Optogenetic stimulation of
496 kisspeptin neurones within the posterodorsal medial amygdala increases luteinising
497 hormone pulse frequency in female mice. J Neuroendocrinol. 2020;32(2):e12823.
498 27. Govic A, Paolini AG. In vivo electrophysiological recordings in amygdala subnuclei
499 reveal selective and distinct responses to a behaviorally identified predator odor. J
500 Neurophysiol. 2015;113(5):1423–36.
501 28. Kinsey-Jones JS, Li XF, Knox AM, Lin YS, Milligan SR, Lightman SL, O'Byrne KT .
502 Corticotrophin-releasing factor alters the timing of puberty in the female rat. J
503 Neuroendocrinol. 2010;22(2):102–9.
504 29. Shemesh Y, Forkosh O, Mahn M, Anpilov S, Sztainberg Y, Manashirov S,

505 Shlapobersky T, Elliott E, Tabouy L, Ezra G, Adler ES . Ucn3 and CRF-R2 in the
506 medial amygdala regulate complex social dynamics. Nat Neurosci. 2016;19(11):1489–
507 96.
508 30. Jamieson PM, Li C, Kukura C, Vaughan J, Vale W. Urocortin 3 modulates the
509 neuroendocrine stress response and is regulated in rat amygdala and hypothalamus by
510 stress and glucocorticoids. Endocrinology. 2006;147(10):4578–88.
511 31. Yeo SH, Kyle V, Morris PG, Jackman S, Sinnett-Smith LC, Schacker M, Chen C,
512 Colledge WH . Visualisation of Kiss1 Neurone Distribution Using a Kiss1-CRE
513 Transgenic Mouse. J Neuroendocrinol. 2016;28(11).
514 32. Paxinos G, Franklin KB . Mouse Brain in Stereotaxic Coordinates. Acad Press.
515 2019;5:246.
516 33. Zhan J, Komal R, Keenan WT, Hattar S, Fernandez DC . Non-invasive strategies for
517 chronic manipulation of dreadd-controlled neuronal activity. J Vis Exp.
518 2019;2019(150):e59439.
519 34. Steyn FJ, Wan Y, Clarkson J, Veldhuis JD, Herbison AE, Chen C. Development of a
520 methodology for and assessment of pulsatile luteinizing hormone secretion in juvenile
521 and adult male mice. Endocrinology. 2013;154(12):4939–45.
522 35. Vidal A, Zhang Q, Médigue C, Fabre S, Clément F. Dynpeak: An algorithm for pulse
523 detection and frequency analysis in hormonal time series. PLoS One.
524 2012;7(7):e39001.
525 36. Fernandes C, File SE. The influence of open arm ledges and maze experience in the
526 elevated plus-maze. Pharmacol Biochem Behav. 1996;54(1):31–40.
527 37. Adekunbi DA, Li XF, Lass G, Shetty K, Adegoke OA, Yeo SH, Colledge WH,
528 Lightman SL, O'Byrne KT. Kisspeptin neurones in the posterodorsal medial amygdala
529 modulate sexual partner preference and anxiety in male mice. J Neuroendocrinol.

530 2018;30(3):e12572.
531 38. Gaytan F, Morales C, Leon S, Heras V, Barroso A, Avendaño MS, Vazquez MJ,
532 Castellano JM, Roa J, Tena-Sempere M . Development and validation of a method for
533 precise dating of female puberty in laboratory rodents: The puberty ovarian maturation
534 score (Pub-Score). Sci Rep. 2017;7(1):1–11.
535 39. Clarkson J, Herbison AE. Postnatal development of kisspeptin neurons in mouse
536 hypothalamus; sexual dimorphism and projections to gonadotropin-releasing hormone
537 neurons. Endocrinology. 2006;147(12):5817–25.
538 40. Clarkson J, Herbison AE. Postnatal development of kisspeptin neurons in mouse
539 hypothalamus; sexual dimorphism and projections to gonadotropin-releasing hormone
540 neurons. Endocrinology. 2006;147(12):5817–25.
541 41. Clarkson J, Boon WC, Simpson ER, Herbison AE. Postnatal Development of an
542 Estradiol-Kisspeptin Positive Feedback Mechanism Implicated in Puberty Onset.
543 Endocrinology. 2009;150(7):3214–20.
544 42. Hu MH, Li XF, McCausland B, Li SY, Gresham R, Kinsey-Jones JS, Gardiner JV,
545 Sam AH, Bloom SR, Poston L, Lightman SL . Relative importance of the arcuate and
546 anteroventral periventricular kisspeptin neurons in control of puberty and reproductive
547 function in female rats. Endocrinology. 2015;156(7):2619–31.
548 43. Kenyon PR, Viñoles C, Morris ST. Effect of teasing by the ram on the onset of puberty
549 in Romney ewe lambs. New Zeal J Agric Res. 2012;55(3):283–91.
550 44. Fabre-Nys C, Cognié J, Dufourny L, Ghenim M, Martinet S, Lasserre O, Lomet D,
551 Millar RP, Ohkura S, Suetomi Y . The two populations of kisspeptin neurons are
552 involved in the ram-induced lh pulsatile secretion and lh surge in anestrous ewes.
553 Endocrinology. 2017;158(11):3914–28.
554 45. Gelez H, Fabre-Nys C . Neural pathways involved in the endocrine response of

555 anestrous ewes to the male or its odor. Neuroscience. 2006;140(3):791–800.
556 46. Pineda R, Plaisier F, Millar RP, Ludwig M. Amygdala Kisspeptin Neurons: Putative
557 Mediators of Olfactory Control of the Gonadotropic Axis. Neuroendocrinology.
558 2017;104(3):223–38.
559 47. Gill JC, Navarro VM, Kwong C, Noel SD, Martin C, Xu S, Clifton DK, Carroll RS,
560 Steiner RA, Kaiser UB . Increased Neurokinin B (Tac2) Expression in the Mouse
561 Arcuate Nucleus Is an Early Marker of Pubertal Onset with Differential Sensitivity to
562 Sex Steroid-Negative Feedback than Kiss1. Endocrinology. 2012;153(10):4883.
563 48. Simavli S, Thompson IR, Maguire CA, Gill JC, Carroll RS, Wolfe A, Kaiser UB,
564 Navarro VM . Substance P Regulates Puberty Onset and Fertility in the Female
565 Mouse. Endocrinology. 2015;156(6):2313–22.
566 49. Wright H, Aylwin CF, Toro CA, Ojeda SR, Lomniczi A . Polycomb represses a gene
567 network controlling puberty via modulation of histone demethylase Kdm6b
568 expression. Sci Rep. 2021;11(1):1–7.
569 50. Comninos AN, Anastasovska J, Sahuri-Arisoylu M, Li XF, Li S, Hu M, Jayasena CN,
570 Ghatei MA, Bloom SR, Matthews PM, O'Byrne KT . Kisspeptin signaling in the
571 amygdala modulates reproductive hormone secretion. Brain Struct Funct.
572 2016;221(4):2035–47.
573 51. Pincus M, Godfrey JR, Feczko E, Earl E, Miranda-Dominguez O, Fair D, Wilson ME,
574 Sanchez MM, Kelly C . Chronic psychosocial stress and experimental pubertal delay
575 affect socioemotional behavior and amygdala functional connectivity in adolescent
576 female rhesus macaques. Psychoneuroendocrinology. 2021;127:105154.
577 52. Yang JA, Song CI, Hughes JK, Kreisman MJ, Parra RA, Haisenleder DJ, Kauffman
578 AS, Breen KM . Acute psychosocial stress inhibits LH pulsatility and kiss1 neuronal
579 activation in female mice. Endocrinology. 2017;158(11):3716–23.

580 53. Marshall AD . Developmental timing of trauma exposure relative to puberty and the
581 nature of psychopathology among adolescent girls. J Am Acad Child Adolesc
582 Psychiatry. 2016;55(1):25–32.
583 54. Johnson FK, Delpech JC, Thompson GJ, Wei L, Hao J, Herman P, Hyder F, Kaffman
584 A . Amygdala hyper-connectivity in a mouse model of unpredictable early life stress.
585 Transl Psychiatry. 2018;8(1):1–14.
586 55. Lin Y, Li XF, Lupi M, Kinsey-Jones JS, Shao B, Lightman SL, O'Byrne KT . The role
587 of the medial and central amygdala in stress-induced suppression of pulsatile LH
588 secretion in female rats. Endocrinology. 2011;152(2):545–55.
589 56. Dopfel D, Perez PD, Verbitsky A, Bravo-Rivera H, Ma Y, Quirk GJ, Zhang N .
590 Individual variability in behavior and functional networks predicts vulnerability using
591 an animal model of PTSD. Nat Commun. 2019;10(1):1–2.
592 57. Chester JA, Barrenha GD, Hughes ML, Keuneke KJ . Age- and sex-dependent effects
593 of footshock stress on subsequent alcohol drinking and acoustic startle behavior in
594 mice selectively bred for high-alcohol preference. Alcohol Clin Exp Res.
595 2008;32(10):1782–94.
596 58. Kinsey-Jones JS, Li XF, Knox AM, Wilkinson ES, Zhu XL, Chaudhary AA, Milligan
597 SR, Lightman SL, O'byrne KT . Down-regulation of hypothalamic kisspeptin and its
598 receptor, Kiss1r, mRNA expression is associated with stress-induced suppression of
599 luteinising hormone secretion in the female rat. J Neuroendocrinol. 2009;21(1):20–9.
600 59. Agnieszka Podfigurna, Anna Szeliga BM. Serum kisspeptin and corticotropin-
601 releasing hormone levels in patients with functional hypothalamic amenorrhea.
602 Gynecol Reprod Endocrinol Metab. 2020;1(1):37–42.
603 60. Li XF, Bowe JE, Lightman SL, O'Byrne KT . Role of corticotropin-releasing factor
604 receptor-2 in stress-induced suppression of pulsatile luteinizing hormone secretion in

605 the rat. Endocrinology. 2005;146(1):318–22.
606 61. Fekete ÉM, Zhao Y, Li C, Sabino V, Vale WW, Zorrilla EP. Social defeat stress
607 activates medial amygdala cells that express type 2 corticotropin-releasing factor
608 receptor mRNA. Neuroscience. 2009;162(1):5–13.
609 62. Pardo-Bellver C, Cádiz-Moretti B, Novejarque A, Martínez-García F, Lanuza E.
610 Differential efferent projections of the anterior, posteroventral, and posterodorsal
611 subdivisions of the medial amygdala in mice. Front Neuroanat. 2012;6(33):1–26.
612 63. Stephens SBZ, Raper J, Bachevalier J, Wallen K. Neonatal amygdala lesions advance
613 pubertal timing in female rhesus macaques. Psychoneuroendocrinology. 2015;51:307–
614 17.
615 64. Deussing JM, Breu J, Kühne C, Kallnik M, Bunck M, Glasl L, Yen YC, Schmidt MV,
616 Zurmühlen R, Vogl AM, Gailus-Durner V . Urocortin 3 modulates social
617 discrimination abilities via corticotropin-releasing hormone receptor type 2. J
618 Neurosci. 2010;30(27):9103–16.
619 65. Cavalcante JC, Sita LV, Mascaro MB, Bittencourt JC, Elias CF. Distribution of
620 urocortin 3 neurons innervating the ventral premammillary nucleus in the rat brain.
621 Brain Res. 2006;1089(1):116–25.
622 66. Li C, Vaughan J, Sawchenko PE, Vale WW. Urocortin III-immunoreactive projections
623 in rat brain: Partial overlap with sites of type 2 corticotrophin-releasing factor receptor
624 expression. J Neurosci. 2002;22(3):991–1001.
625 67. Day FR, Elks CE, Murray A, Ong KK, Perry JRB. Puberty timing associated with
626 diabetes, cardiovascular disease and also diverse health outcomes in men and women:
627 the UK Biobank study. Sci Rep. 2015;5(1):1–12.
628

629 **Figure 1.** DREADD activation of kisspeptin (kiss1) neurons in the posterodorsal sub-nucleus
630 of the medial amygdala (MePD) from post-natal day (pnd) 21 for 14 days advances first estrous
631 (FE) without affecting vaginal opening (VO) and body weight (BW) in Kiss-cre-tdTomato
632 female mice. Effect of MePD kiss1 activation on day of VO (A), FE (B) and (C) BW weight
633 gain between pnd 21 and 45. +$p<0.05$ Control group (combined control AAV: n=5; no surgery:
634 n=5) vs DREADD group (n=8).

635 **Figure 2.** Chronic 2,4,5-Trimethylthiazole (TMT) exposure from post-natal day (pnd) 21 for
636 14 days delays first estrous (FE) without affecting vaginal opening (VO) and body weight
637 (BW) in C57Bl6/J female mice. Effect of chronic TMT exposure on day of VO (A), FE (B)
638 and (C) BW weight gain between pnd 21 and 45. +++$p<0.0001$ Control group (combined
639 water control: n=6; ethyl vanillin control: n=4) vs TMT group (n=14).

640 **Figure 3.** Chronic 2,4,5-Trimethylthiazole (TMT) exposure from post-natal day (pnd) 21 for
641 14 days suppresses pre-pubertal pulsatile luteinising hormone (LH) secretion on pnd 26 and 29
642 in C57Bl6/J female mice. Representative LH pulse profile with (A) control mouse on pnd 26,
643 (B) TMT-exposed mouse on pnd 26, (C) control mouse on pnd 29 and (D) TMT-exposed
644 mouse on pnd 29. (E), Summary of LH pulse frequency on pnd 26 and 29 of control and TMT-
645 exposed group during the 80 min blood sampling period. LH pulses detected by the DynePeak
646 algorithm are indicated with an asterisk located above each pulse on the representative LH
647 pulse profiles. ++$p<0.001$ control group (combined water control: n=6; ethyl vanillin control:
648 n=3) vs. TMT-exposed group (n=8) on pnd 26 and 29.

649 **Figure 4.** Chronic 2,4,5-Trimethylthiazole **(**TMT) exposure increased anxiety-like behavior
650 on the light-dark box (LDB) and elevated plus maze (EPM) and decreased social interaction
651 with familiar conspecifics on the social interaction (SI) test. (A) Summary of time spent in the

652 light compartment of the LDB on post-natal day (pnd) 19 (before beginning of TMT-exposure),
653 27 (during TMT exposure) and 40 (after termination of TMT-exposure), (B) time spent socially
654 interacting with familiar conspecifics on pnd 19, 27 and 40, and (C) time spent in the open arm
655 of the EPM on pnd 20, 28 and 41. +p<0.05 time spent on LDB, SI and EPM of control group
656 (combined water control: n=6; ethyl vanillin control: n=4) vs TMT-exposed group (n=14) on
657 pnd 27 or 28 (during TMT-exposure); ###p<0.0001 time spent in the open arm of the EPM in
658 the TMT-exposed group on pnd 28 vs pnd 41.

659 **Figure 5.** DREADD activation of urocortin 3 (Ucn3) neurons in the posterodorsal sub-nucleus
660 of the medial amygdala (MePD) from post-natal day (pnd) 21 for 14 days delays first estrous
661 (FE) without affecting vaginal opening (VO) and body weight (BW) in urocortin3-cre-
662 tdTomato female mice. Effect of MePD Ucn3 activation on day of VO (A), FE (B) and (C)
663 BW weight gain between pnd 21 and 45. +p<0.05 Control group (combined control AAV: n=6;
664 no surgery: n=4) vs DREADD group (n=8).

665 **Figure 6.** Expression of AAV5-hSyn-DIO-HA-hM3D(Gq)-IRES-mCitrine in posterodorsal
666 medial amygdala (MePD) Kisspeptin (kiss1) neurons. (A-F) Representative dual fluorescence
667 photomicrographs of the MePD from a Kiss-cre-tdTomato female mouse injected with AAV5-
668 hSyn-DIO-HA-hM3D(Gq)-IRES-mCitrine. kiss1 neurons labelled with m-Citrine (A) and
669 tdTomato (C) appear yellow/orange (E). (B), (D) and (F) are a higher power view of (A), (C)
670 and (E) respectively. Scale bars represent A, C, E 100 μm and B, D, F 25 μm; OT, Optic tract
671 (blue line).

672 **Figure 7.** Expression of AAV5-hSyn-DIO-HA-hM3D(Gq)-IRES-mCitrine in posterodorsal
673 medial amygdala (MePD) Urocortin 3 (Ucn3) neurons. (A-F) Representative dual fluorescence
674 photomicrographs of the MePD from a Ucn3-cre-tdTomato female mouse injected with

675 AAV5-hSyn-DIO-HA-hM3D(Gq)-IRES-mCitrine. Ucn3 neurons labelled with m-Citrine (A)
676 and tdTomato (C) appear yellow/orange (E). (B), (D) and (F) are a higher power view of (A),
677 (C) and (E) respectively. Scale bars represent A, C, E 100 μm and B, D, F 25 μm; OT, Optic
678 tract (blue line).

Figure 1

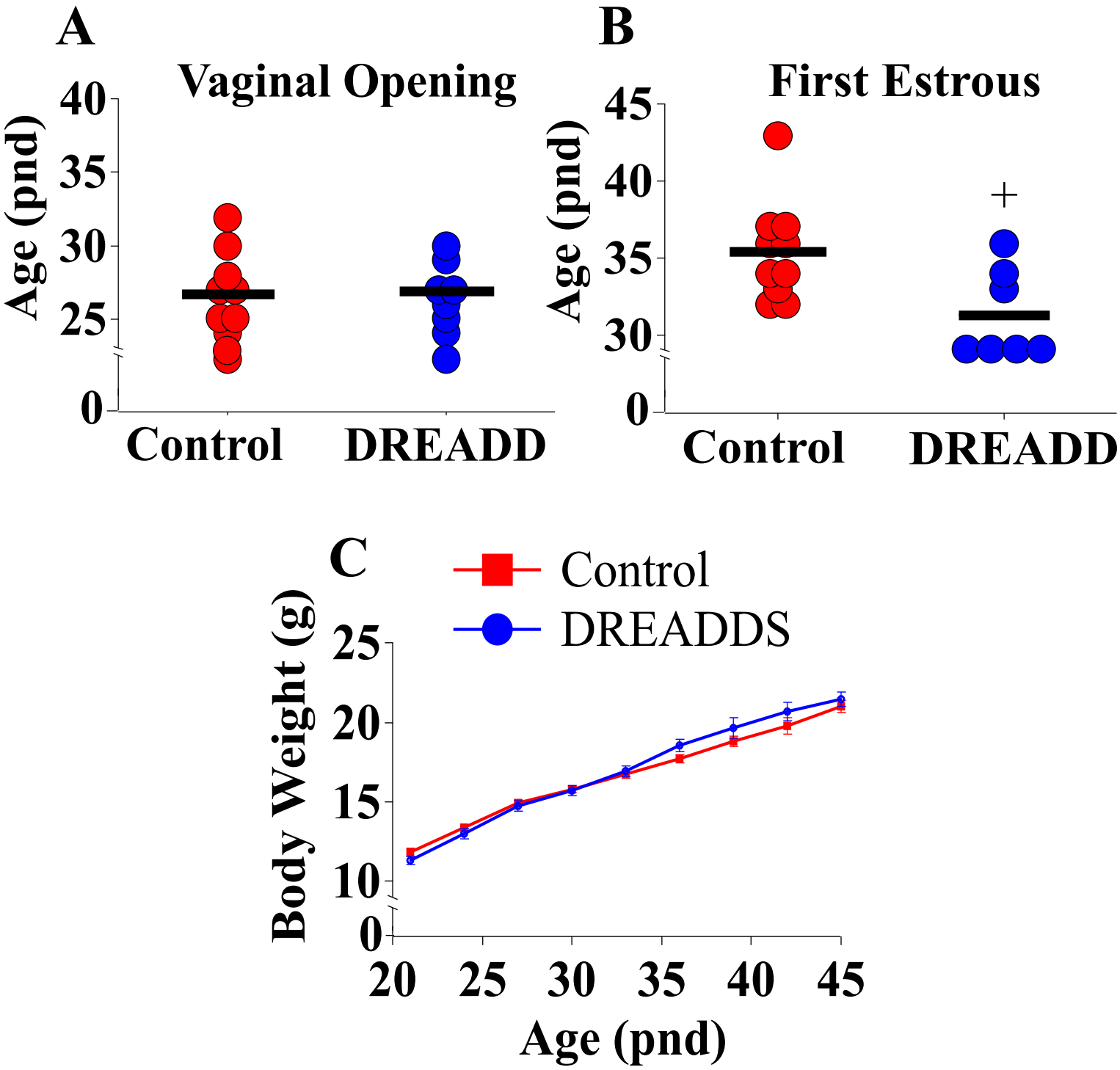
A
Vaginal Opening
Age (pnd)
40
35
30
25
0
Control
DREADD
B
First Estrous
Age (pnd)
45
40
35
30
0
+
Control
DREADD
C
Control
DREADDS
Body Weight (g)
25
20
15
10
0
20
25
30
35
40
45
Age (pnd)

Figure 2

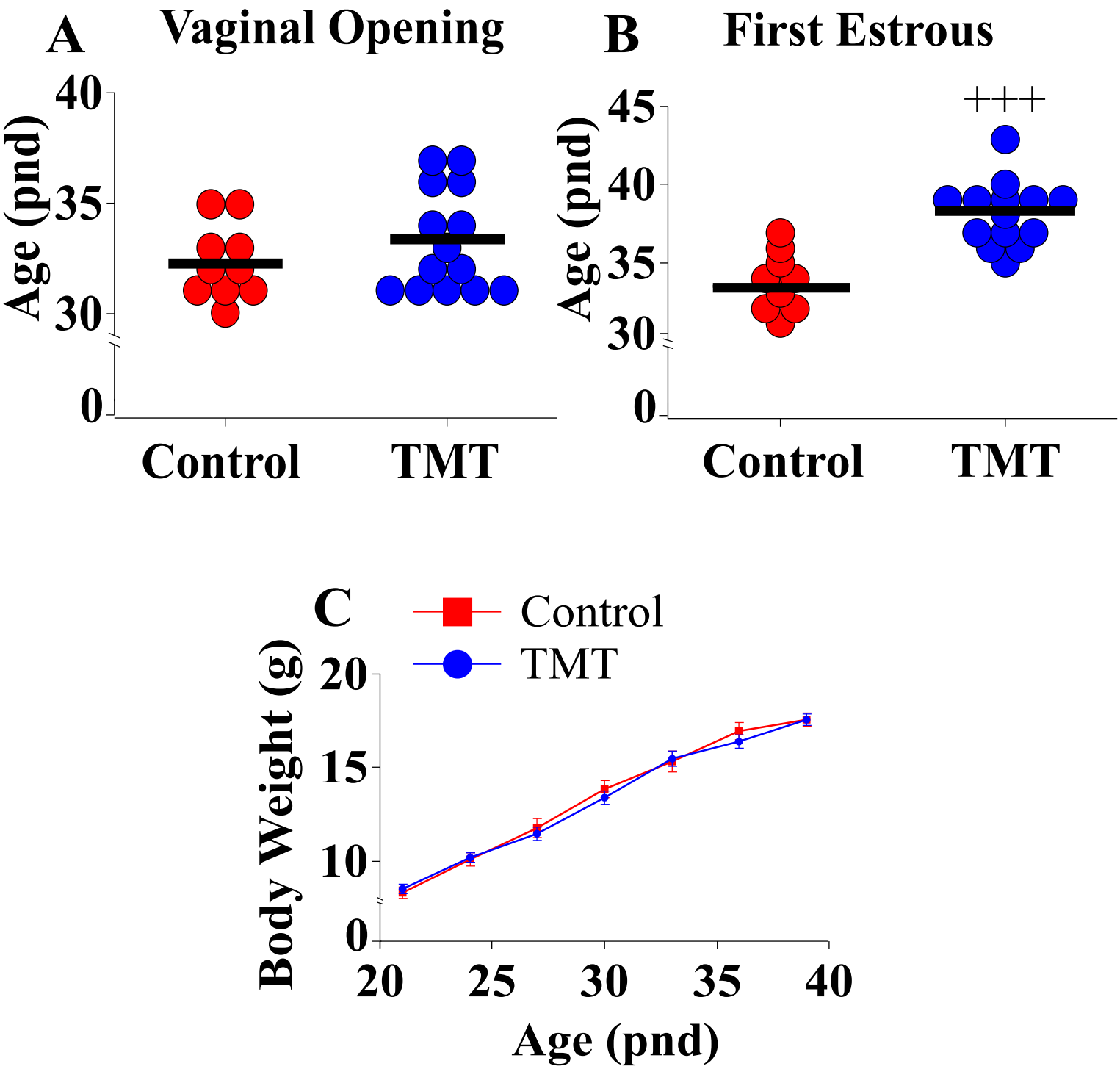
A
Vaginal Opening
Age (pnd)
40
35
30
0
Control
TMT
B
First Estrous
Age (pnd)
45
40
35
30
0
+++
Control
TMT
C
Control
TMT
Body Weight (g)
20
15
10
0
20
25
30
35
40
Age (pnd)

Figure 3

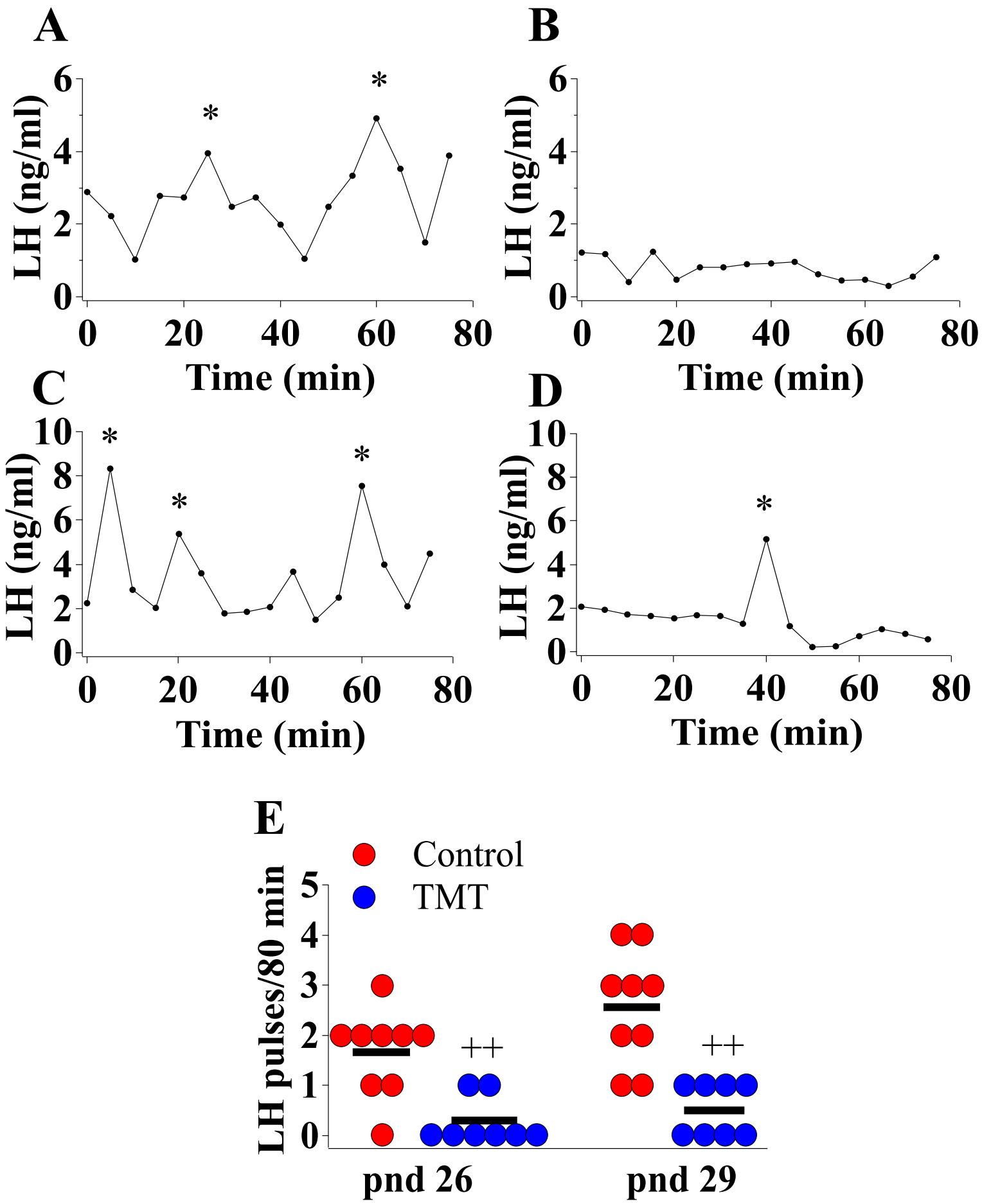
A
B
C
D
E
LH (ng/ml)
Time (min)
LH pulses/80 min
Control
TMT
++
pnd 26
pnd 29

Figure 4

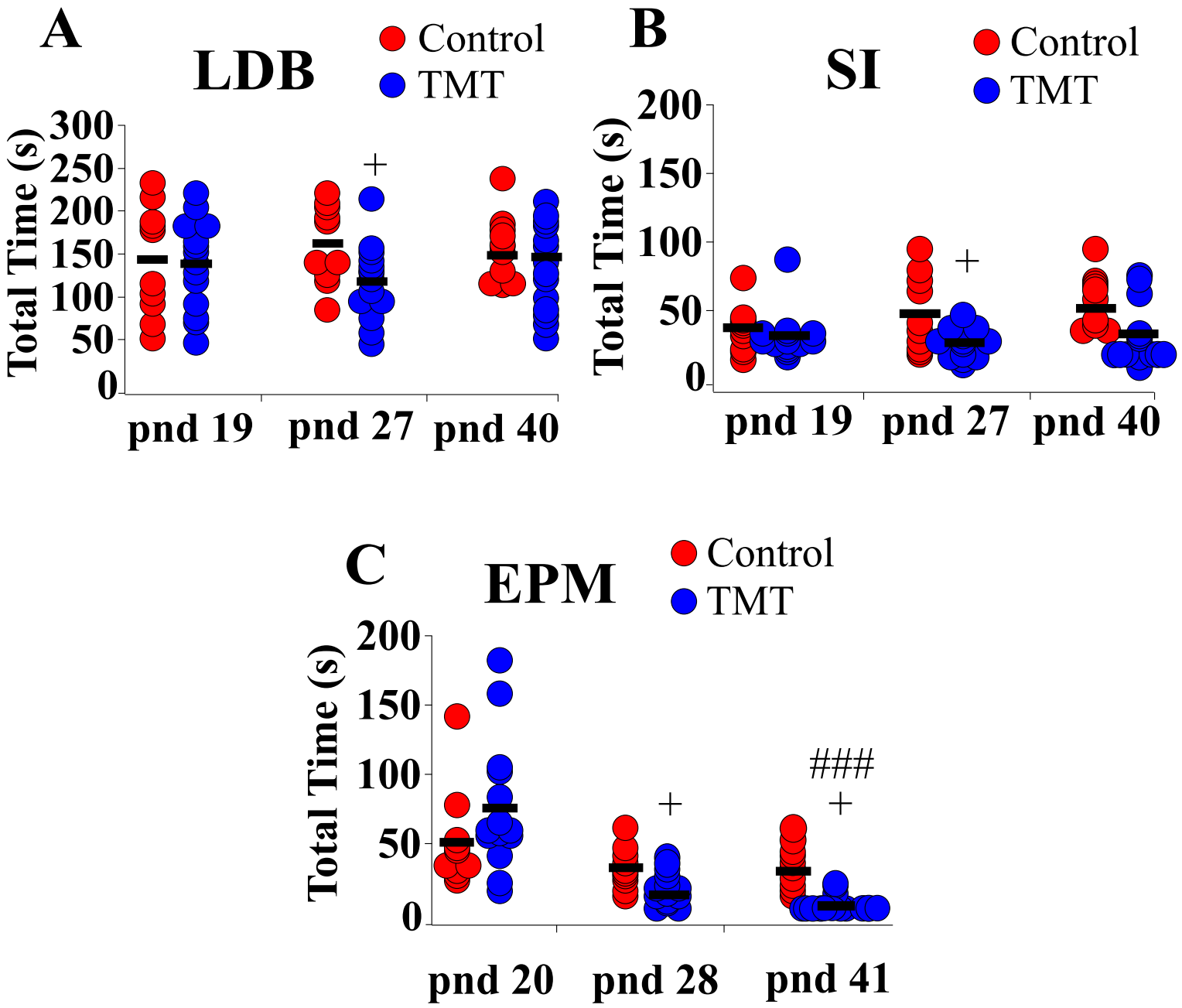
A
LDB
Control
TMT
Total Time (s)
300
250
200
150
100
50
0
+
pnd 19
pnd 27
pnd 40
B
SI
Control
TMT
Total Time (s)
200
150
100
50
0
+
pnd 19
pnd 27
pnd 40
C
EPM
Control
TMT
Total Time (s)
200
150
100
50
0
+
###
+
pnd 20
pnd 28
pnd 41

Figure 5

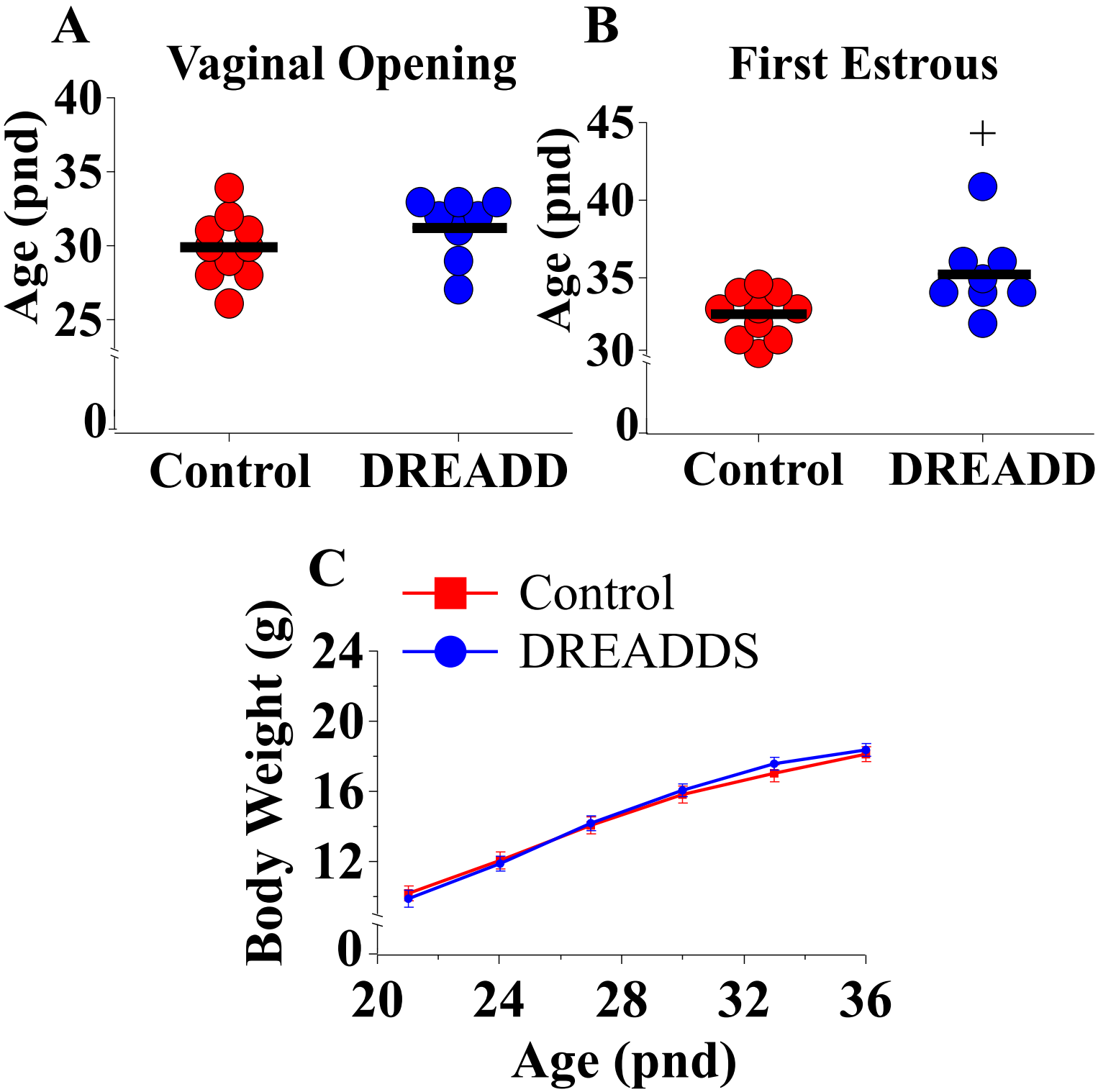
A
Vaginal Opening
Age (pnd)
40
35
30
25
0
Control
DREADD
B
First Estrous
Age (pnd)
45
40
35
30
0
+
Control
DREADD
C
Control
DREADDS
Body Weight (g)
24
20
16
12
0
20
24
28
32
36
Age (pnd)

Figure 6

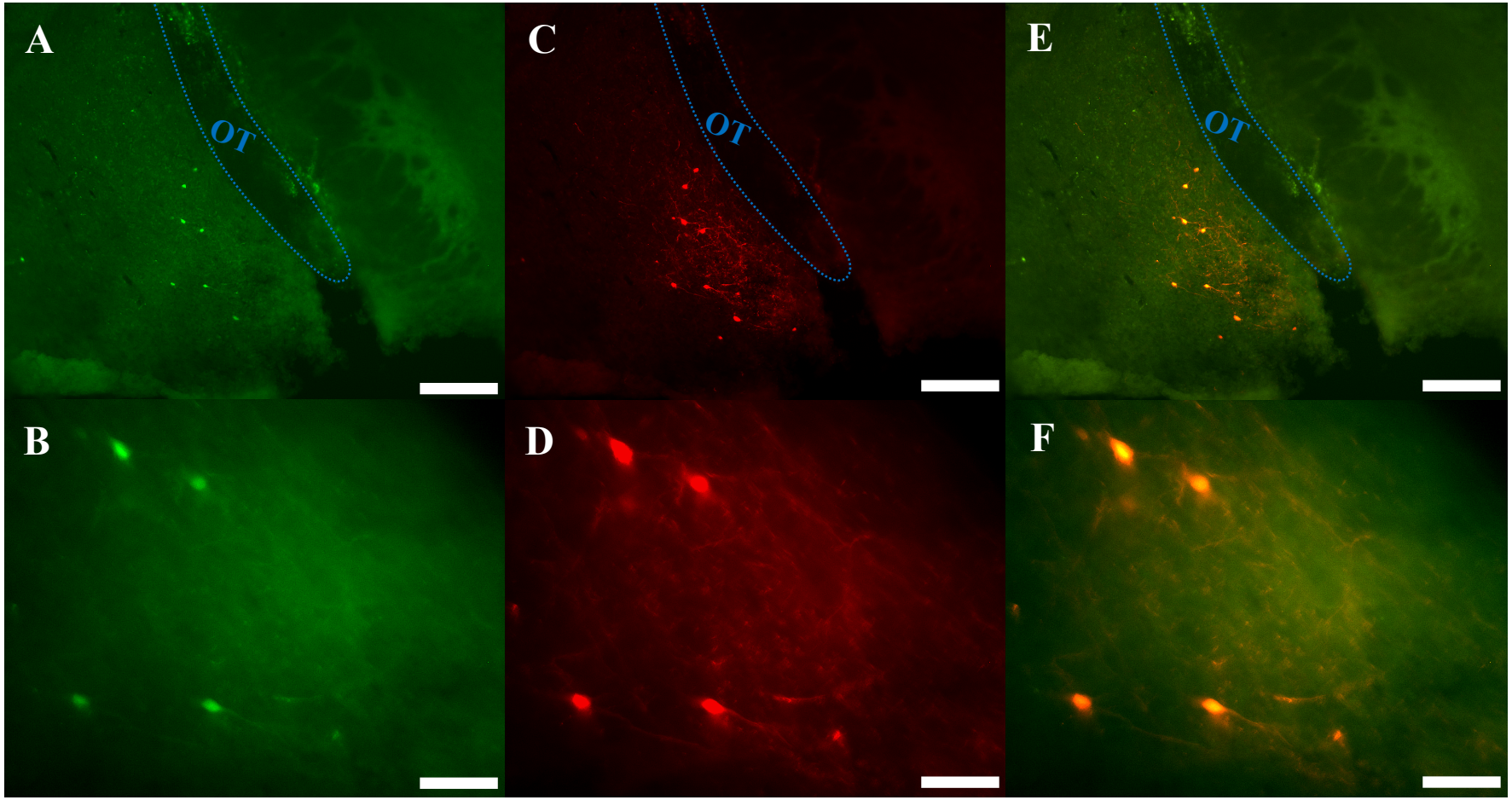
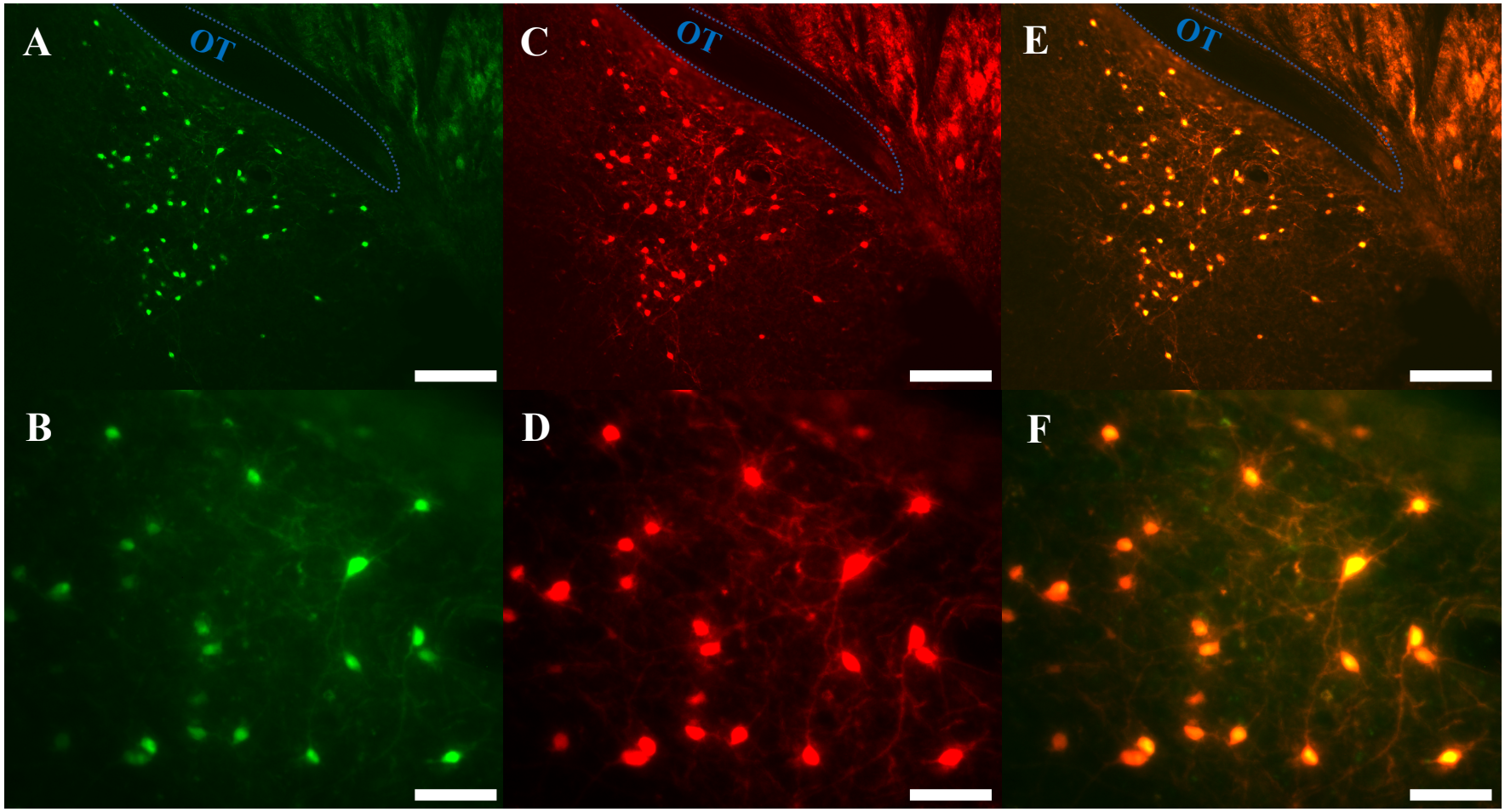
Figure 7